Chemomechanical synchronization in heterogeneous self-oscillating gels

Victor V. Yashin and Anna C. Balazs*

Chemical Engineering Department, University of Pittsburgh, Pittsburgh, Pennsylvania 15261, USA

(Received 6 September 2007; revised manuscript received 3 December 2007; published 15 April 2008)

Using computational modeling, we introduce patches of self-oscillating gels undergoing the Belousov-Zhabotinsky (BZ) reaction into a nonreactive polymer network and thereby demonstrate how these BZ gels can be harnessed to impart remarkable functionality to the entire system. By first focusing on two adjacent patches of BZ gels, we show that the patches' oscillations can become synchronized in phase or out of phase, with the oscillation frequency depending on the synchronization mode and the spatial separation between these domains. We then apply these results to an array of five adjacent BZ patches and by varying the distance between these pieces, we dramatically alter the dynamical behavior of the patterned gel. For example, the sample can be made to exhibit a unidirectional traveling wave or display a concerted expansion and contraction, properties that are valuable for creating gel-based devices, such as micropumps and microactuators. The findings point to a "modular" design approach, which can impart different functionality simply by arranging identical pieces of BZ gels into distinct spatial arrangements within a polymer matrix.

DOI: 10.1103/PhysRevE.77.046210 PACS number(s): 47.54.−r, 82.40.Bj

I. INTRODUCTION

One of the grand challenges in designing flexible robots or "soft machines" is to create a system that can operate under its own, internally generated power, similar to a living system [1,2]. Recently, researchers have made significant progress towards this goal by fabricating a polymer gel that undergoes spontaneous, periodic oscillations [2,3], which are driven by the Belousov-Zhabotinsky (BZ) reaction [4]. The gel will continue to undergo a rhythmic swelling and deswelling until the reagents in the BZ reaction are consumed; the system can, however, be "refueled" by simply adding more reagents to the solvent. The unique self-oscillatory behavior of the BZ gels is due to a ruthenium catalyst, which is grafted to the backbone of the polymers [2,3]. The metal catalyst ions undergo a periodic reduction and oxidation and this redox reaction drives the rhythmic expansion and contraction of the polymer. By exploiting this form of chemomechanical transduction, researchers could design various self-propelled BZ gels [1,5,6].

Recent theoretical and computational modeling of BZ gels has revealed a number of distinctive effects of the chemomechanical coupling on the dynamical behavior of the polymer network [5–8]. For example, computer simulations of the BZ gel in two dimensions (2D) uncovered a rich variety of dynamic patterns and distinctive shape changes that depend on the aspect ratio of the sample, and exist solely due to coupling between the chemical and mechanical degrees of freedom [7]. Anchoring the BZ gel to a solid wall was shown to yield different dynamic patterns depending on whether the gel was expanded or contracted near the wall, and on the sample's dimensions [5]. Additionally, it was found that applying a mechanical pressure on a sample could induce oscillations in an initially nonoscillatory system or promote changes in existing oscillatory patterns [6]. Finally, researchers isolated scenarios where the traveling waves of swelling induce a microscopic motion of the entire sample [5,6].

In the previous studies, the gels were assumed to contain a uniform distribution of the anchored metal catalyst. In this paper, we examine how chemical patterning can be harnessed to expand the functionality of the BZ gels. In particular, we use computational modeling to probe the behavior of BZ gels where only finite patches in the sample contain the Ru catalyst (BZ patches). As we show below, a pair of isolated BZ patches exhibits two modes of synchronization of the chemomechanical oscillations, with the frequency of these oscillations being strongly dependent on the interpatch distance. We then demonstrate that this finding could be utilized for creating organizing centers, or pacemakers, within heterogeneous gels that consist of many identical BZ patches. Thus, this kind of a spatial heterogeneity leads not only to unique pattern formation, but also opens up a method of tailoring the gels for specific applications.

II. METHODOLOGY

A. Model description

We start by considering the system shown schematically in Fig. 1(a): two square patches of BZ gels (which contain the anchored catalyst) are placed a distance Δx apart within a rectangular layer of swollen, nonreactive gel. To describe the dynamics within the BZ gel, we turn to our modified version [5,8] of the Oregonator model [9], which captures the reaction in solution in terms of the concentrations of the key reaction intermediate (the activator) u, and the oxidized metal-ion catalyst v. Our modified model [5,8] accounts for the dependence of the BZ reaction rates on the volume fraction of polymer ϕ, yielding the following dimensionless reaction-diffusion equations for u and v, and the continuity equation for ϕ:

$$\frac{\partial u}{\partial t} = -\nabla \cdot (u\mathbf{v}^{(s)}) - \nabla \cdot \mathbf{j}^{(u)} + F(u,v,\phi), \qquad (1)$$

*Corresponding author; balazs1@engr.pitt.edu

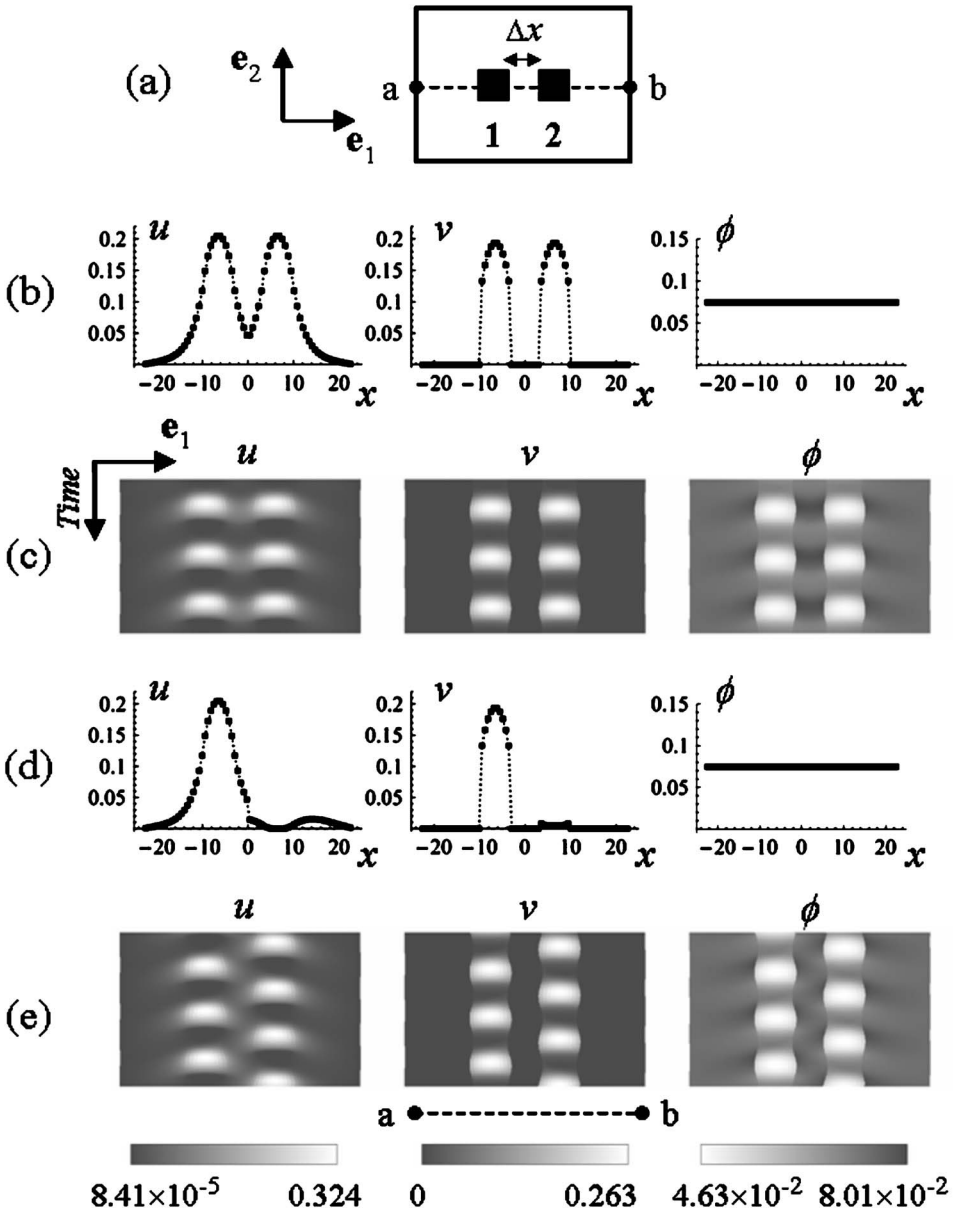

FIG. 1. Synchronization modes in the patterned BZ gel. (a) Schematics of the system in the nondeformed state; the black squares denote the catalyst patches 1 and 2. (b) The initial conditions corresponding to $\Delta\theta=0$. (c) The in-phase synchronization. (d) The initial conditions corresponding to $\Delta\theta=\pi$. (e) The out-of-phase synchronization. Here and in all other figures, the patch size is $5L_0$ and the patch-to-boundary distance is $10L_0$; the sample swells freely through the outer boundaries; $u=0$ outside the sample. The spatiotemporal behavior of u, v, and ϕ was obtained at $\Delta x=5L_0$ and $\chi^*=0.105$, and shown along the cross section a-b. The gel dynamics is shown during the period of time of $100T_0$. The lattice spacing in the simulations is $1/2L_0$. The symbols in (b) and (d) present the values of u, v, and ϕ at the center of elements; the symbols are connected by dotted lines as a guide for the eye.

$$\frac{\partial v}{\partial t} = -\nabla \cdot (v\mathbf{v}^{(p)}) + \varepsilon G(u,v,\phi), \tag{2}$$

$$\frac{\partial \phi}{\partial t} = -\nabla \cdot (\phi\mathbf{v}^{(p)}). \tag{3}$$

Here, $\mathbf{v}^{(s)}$ and $\mathbf{v}^{(p)}$ are the respective solvent and polymer velocities, $\mathbf{j}^{(u)}$ is the diffusion flux of the dissolved activator, and F and G are the BZ reaction rate functions. Equation (2) only applies to the BZ patches, where the catalyst is chemically bonded to the polymer chains. Within these patches, the reaction rates F and G are [5,8]

$$F(u,v,\phi) = (1-\phi)^2 u - u^2 - (1-\phi) f v \frac{u - q(1-\phi)^2}{u + q(1-\phi)^2}, \tag{4}$$

$$G(u,v,\phi) = (1-\phi)^2 u - (1-\phi) v. \tag{5}$$

The stoichiometric factor f and the dimensionless parameters ε and q have the same meaning as in the original Oregonator [9]. Outside the BZ patches, u decays through a second-order reaction, so $F(u,v,\phi)=-u^2$ in the nonreactive regions. Aside from incorporating the effects of the polymer, a similar approach has been used to model the BZ reaction in chemically patterned media [10].

We neglect the total velocity of the polymer-solvent system by assuming, for simplicity, that the gel dynamics proceeds solely due to polymer-solvent interdiffusion, and set $\phi\mathbf{v}^{(p)}+(1-\phi)\mathbf{v}^{(s)}=0$. In the course of interdiffusion, the forces that act on the deformed gel are balanced by the frictional drag due to the motion of the solvent [11,12]. Then, the polymer velocity can be calculated as [12] $\mathbf{v}^{(p)}=\Lambda_0(1-\phi)(\phi/\phi_0)^{-3/2}\nabla\cdot\hat{\boldsymbol{\sigma}}$, where $\hat{\boldsymbol{\sigma}}$ and Λ_0 are the respective dimensionless stress tensor and kinetic coefficient, and the fac-

tor $(\phi/\phi_0)^{-3/2}$ is due to the ϕ-dependent polymer-solvent friction.

To determine the properties of the system [i.e., solve the set of equations in (1)–(3)], we must be able to calculate the stresses in the system. The stresses in the polymer network depend on the local deformations, which are described by the Finger strain tensor $\hat{\mathbf{B}}$ [13]. The stress-strain relationship can be established from the energy density of the deformed gel U. The energy density depends on the strain tensor $\hat{\mathbf{B}}$ only through it's invariants I_i, $i=1,2,3$. Given that the function $U(I_1,I_2,I_3)$ is specified, the stress tensor $\hat{\boldsymbol{\sigma}}$ can be calculated as [13]

$$\hat{\boldsymbol{\sigma}} = 2I_3^{-1/2}(w_2 I_2 + w_3 I_3)\hat{\mathbf{I}} + 2I_3^{-1/2} w_1 \hat{\mathbf{B}} - 2I_3^{1/2} w_2 \hat{\mathbf{B}}^{-1}, \quad (6)$$

where $w_i=(\partial/\partial I_i)U(I_1,I_2,I_3)$, $i=1,2,3$, and $\hat{\mathbf{I}}$ is the unit tensor. In our calculations, the quantity U is taken to be the sum of the elastic energy of the crosslinked polymer chains, the polymer-solvent interaction energy, and the energy of catalyst-solvent interactions [5,8] as follows:

$$U = U_{el}(I_1,I_3) + U_{FH}(I_3) + U_{cpl}(I_3). \quad (7)$$

The corresponding strain invariants are $I_1=\mathrm{tr}\,\hat{\mathbf{B}}$ and $I_3=\det\hat{\mathbf{B}}$. To calculate the elastic energy, we utilize the Flory model of rubber elasticity

$$U_{el} = \frac{c_0}{2}(I_1 - 3 - \ln I_3^{1/2}), \quad (8)$$

where c_0 is the dimensionless crosslink density of the gel. The polymer-solvent interactions are described according to the Flory-Huggins model

$$U_{FH} = I_3^{1/2}[(1-\phi)\ln(1-\phi) + \chi_{FH}(\phi)\phi(1-\phi)], \quad (9)$$

where $\chi_{FH}(\phi)$ is the ϕ-dependent polymer-solvent interaction parameter. The coupling between the chemical and mechanical degrees of freedom is introduced by taking the catalyst-solvent interaction energy to be of the following form [5,8]:

$$U_{cpl} = -I_3^{1/2}\chi^* v(1-\phi). \quad (10)$$

Here, $\chi^*>0$ is the interaction parameter that describes the hydrating effect of the oxidized metal-ion catalyst. The factor $I_3^{1/2}$ appears in Eqs. (9) and (10) because the energy density is defined with respect to a unit volume in the undeformed state. We note that the local volume fraction of polymer in the deformed gel ϕ is related to the volume fraction of polymer in the undeformed state ϕ_0, as $\phi=\phi_0 I_3^{-1/2}$. Finally, substituting Eqs. (7)–(10) into Eq. (6) gives the following constitutive equation [5,8]:

$$\hat{\boldsymbol{\sigma}} = -[\pi_{FH}(\phi) + \chi^* v\phi + c_0\phi(2\phi_0)^{-1}]\hat{\mathbf{I}} + c_0\phi_0^{-1}\phi\hat{\mathbf{B}}, \quad (11)$$

where

$$\pi_{FH}(\phi) = -[\phi + \ln(1-\phi) + \chi(\phi)\phi^2] \quad (12)$$

is the dimensionless Flory-Huggins osmotic pressure. The interaction parameter $\chi(\phi)$ in Eq. (12) coincides with the Flory-Huggins interaction parameter χ_{FH} in Eq. (9) only if the polymer-solvent interactions do not depend on the volume fraction of polymer ϕ.

B. Numerical simulations

Equations (1)–(3) were solved numerically using a lattice-based computational technique, namely, the gel lattice spring model [5,7]. These simulations are carried out in two dimensions and thus, the height of the film $\lambda_\perp$ is assumed to remain constant. For the BZ reaction parameters [see Eqs. (2) and (4)], we set $\varepsilon=0.354$, $q=9.52\times10^{-5}$, and $f=0.7$. The polymer gel was characterized by $\phi_0=0.139$, $c_0=1.3\times10^{-3}$, $\Lambda_0=100$, and $\lambda_\perp=1.1$. The polymer- and catalyst-solvent interactions were set to $\chi(\phi)=0.338+0.518\phi$ and $\chi^*=0.105$, respectively. These parameter values were based, where possible, on available experimental data [5]; f and χ^* were treated as the adjustable parameters. The units of time and length used in our simulations correspond to $T_0\sim1$ s and $L_0\sim40$ μm, respectively [5].

To clarify the terminology used below, the BZ patch contains the anchored catalyst and this patch can be responsive ($\chi^*>0$) or nonresponsive ($\chi^*=0$). The bulk of the gel in the ensuing discussion (see Fig. 1) is nonreactive, i.e., no catalyst is anchored to the chains in this region. At the onset, we considered the case where a single BZ patch of the responsive gel ($\chi^*=0.105$) is surrounded by the nonreactive gel (dimensions of both are given below). We found that the responsive patch exhibits oscillations for values of the stoichiometric factor f in the range from 0.659 ± 0.001 to 1.25 ± 0.02. We then considered a similar sized piece of the nonresponsive gel ($\chi^*=0$) in the nonreactive matrix and found that BZ oscillations existed in the range from 0.683 ± 0.001 to 1.25 ± 0.02, i.e., the oscillatory domain for the nonresponsive gel was smaller than in the responsive gel.

Using the above approach, we studied the synchronization of the chemomechanical oscillations of two square-shaped BZ gel patches, which were placed within the nonreactive gel, as shown in Fig. 1(a). The state of synchronization was characterized by the phase difference $\Delta\theta$ between the oscillations of v (concentration of oxidized catalyst) in the center of the two patches. The size of the BZ patches was $5L_0$ and the patch-to-boundary distance was $10L_0$ [see Fig. 1(a)]. The lattice spacing in the simulations was $1/2L_0$. The interpatch distance Δx was varied from $1L_0$ to $10L_0$. The latter dimensions correspond to the undeformed state of the gel. The distance from the BZ patch to the edge of the sample was chosen to be two times greater than the size of the patch in order to minimize the effect of the boundary conditions on the gel dynamics within and around the BZ patches. For the boundary conditions, we assumed the gel sample to swell freely in the lateral direction through the outer sample boundaries, and the concentration of the activator was set to $u=0$ outside the sample.

All simulations were initiated from a gel that was uniformly swollen in the lateral directions. In this initial state, the degree of lateral swelling was set equal to that of a nonreactive gel at equilibrium; the equilibrium degree of lateral swelling of the nonreactive gel is approximately 1.3 for the

given values of the model parameters. The initial spatial distributions of the concentrations of u and v were obtained from a simulation on a single, nonresponsive BZ patch ($\chi^*=0$), which was located in the center of a larger square of nonreactive matrix. (The size of the square BZ patch and the distance of this patch from the edge of the sample are the same as noted above.) The resulting concentration fields for u and v were utilized as the initial distributions in the two BZ patches in the rectangular sample [Fig. 1(a)]. Additionally, the spatial patterns of u and v centered on the different patches were selected so as to exhibit a phase shift, i.e., they corresponded to different positions on the cycle of an individual chemical oscillator. The initial state of patch 1 was typically chosen at a position of maximum of v in the center of the patch. We varied the initial phase difference $\Delta\theta$ from 0 to $7\pi/8$ with a step of $\pi/8$. Figures 1(b) and 1(d) show the profiles of u, v, and ϕ along the central cross section of the sample at $\Delta\theta=0$ and π, respectively.

After assigning the initial conditions, the system dynamics was simulated for a time of $3000T_0$, which is approximately equal to 100 cycles of the BZ reaction. This period of time was sufficiently long to establish synchronized regimes of oscillation for $\Delta x \leq 10$. To facilitate transitions between different synchronization regimes, the system dynamics was then perturbed five consecutive times by applying a random noise to the values of u and v. After each perturbation, the simulation was run for an additional 1000 units of time.

III. RESULTS AND DISCUSSION

Due to the redox reaction of the metal catalyst, the two patches of responsive BZ gels shown in Fig. 1 exhibit periodic oscillations; furthermore, these oscillating patches interact, or effectively "communicate," through the concentration field u and the deformation of the gel around the reactive regions. (In other words, the redox reaction within the two patches is correlated because the activator u diffuses out of one patch and into the other. In this manner, the diffusing activator effectively controls the interaction between the patches.) Due to this interaction, the chemomechanical oscillations in the patches become synchronized [14]. The simulations reveal two major modes of synchronization, namely, in-phase and out-of-phase synchronization. These respective modes are displayed in Figs. 1(c) and 1(e), which show the temporal behavior of u, v, and ϕ along the central cross section of the gel. In a synchronized state, the phase difference between the two oscillators, $\Delta\theta$, is locked to a specific constant value. For the in-phase synchronization [Fig. 1(c)], $\Delta\theta=0$, while for the out-of-phase mode [Fig. 1(e)], the phase difference is about $\Delta\theta=\pi$.

The two modes of synchronization were found to coexist in a wide range of the interpatch distances Δx (see the discussion below). Hence, the mode selection depended upon the initial conditions chosen for the simulations. To achieve the in-phase synchronization illustrated in Fig. 1(c), the simulations were initiated from conditions that correspond to the same phase of oscillation in the individual BZ oscillators as shown in Fig. 1(b). The in-phase mode was also observed if the spatially uniform distributions u and v were used for the initial conditions. The out-of-phase regime shown in Fig. 1(e) was established at the nonequal initial phases [see Fig. 1(d)]. It is worth noting that in experimental studies, the light sensitivity of the BZ reaction could be utilized for manipulating the initial conditions [16–18].

We note that for two patches at $\Delta x=5$, the synchronized oscillations were observed in approximately the same range of values of the stoichiometric factor f as where a single BZ patch exhibited the oscillatory regime, i.e., $0.659 \leq f \leq 1.25$ at $\chi^*=0.105$ and $0.683 \leq f \leq 1.25$ at $\chi^*=0$.

The periodic swelling of the polymer in the BZ patches [the bright spots in the density plots of ϕ in Figs. 1(c) and 1(e)] proceeds through the repetitive uptake and release of solvent from the neighboring areas, causing a distortion of the polymer network that borders these patches. This can clearly be seen in Figs. 2(a) and 2(b), which display the relative variation of ϕ along the central cross section of the sample for both synchronization modes. The variation $\delta\phi$ in Figs. 2(a) and 2(b) is defined as $\delta\phi=\phi-\phi_{eq}$, where ϕ_{eq} is the equilibrium volume fraction of polymer in the nonresponsive gel, i.e., at $\chi^*=0$. The figures also show that the distributions of ϕ within the gel are different for these two modes. This difference can be further characterized by the variation in the energy density of the gel due to the deformations caused by the BZ reaction. The energy density is defined as $U_{gel}=U_{el}+U_{FH}$ [see Eqs. (8) and (9)]. It is convenient to calculate the value $\delta U_{gel}=\bar{U}_{gel}-U_{gel}^{(eq)}$, where $\bar{U}_{gel}$ is the total energy of the gel per unit volume in the nondeformed state, and $U_{gel}^{(eq)}$ is the equilibrium value of U_{gel} in the nonresponsive gel ($\chi^*=0$). Figure 2(c) shows how δU_{gel} varies with time and reveals that the amplitude of its variations is greater for the in-phase than for the out-of-phase mode. The solid and dashed lines in Figs. 2(a) and 2(b) correspond to the maximal and minimal values of δU_{gel}, respectively. As can be seen from these figures, ϕ exhibits more significant spatial variations for the in-phase mode than for the out-of-phase mode.

We now systematically varied the distance between the patches, Δx, while fixing $\chi^*=0.105$ and found that the synchronization between the two oscillators depends critically on Δx. Figure 3(a) shows that only the in-phase mode was found for $\Delta x<3$, whereas both the in-phase and out-of-phase modes were observed for $\Delta x \geq 3$. Furthermore, the frequency of oscillation ω in a synchronized state also depends on Δx, and this dependence is remarkably different for the two modes. In particular, ω in the out-of-phase mode increases as the BZ patches are placed closer together until this mode ceases to exist at $\Delta x<3$. In contrast, ω in the in-phase mode decreases with a decrease in Δx. Moreover, there exists a range of the interpatch distances [$3 \leq \Delta x \leq 6$ in Fig. 3(a)], where the out-of-phase patches oscillate with a higher frequency than the patches exhibiting the in-phase mode.

We anticipate that in the limit that Δx approaches zero, the frequency of the oscillations in the in-phase mode should approach the frequency of oscillation in a single patch, ω_0. To obtain accurate numerical results in this limit, however, the lattice spacing should be taken to be much smaller than in the present study.

As can be seen from Fig. 3(b), the behavior of the chemoresponsive gel ($\chi^*=0.105$) is quite distinct from the nonre-

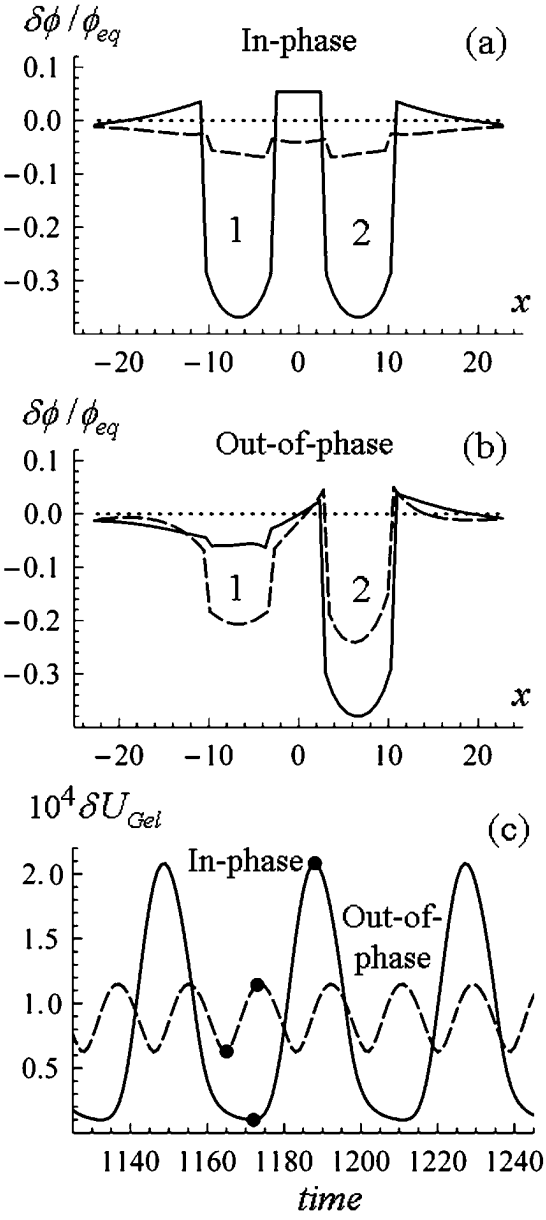

FIG. 2. Distortion of the polymer network in the patterned BZ gel exhibiting the (a) in-phase and (b) out-of-phase synchronization as revealed by the variation in the volume fraction of polymer $\delta\phi$ along the central horizontal cross section at $\Delta x=5L_0$ and $\chi^*=0.105$; ϕ_{eq} corresponds to $\chi^*=0$. (c) The temporal variation of the energy of the gel, δU_{gel}, which is calculated per unit volume of gel in the nondeformed state, and includes the elastic energy of the crosslinked polymer chains and the energy of the polymer-solvent interactions due to the Flory-Huggins equation [5,8]. The solid and dashed lines in (a) and (b) correspond to the profiles of $\delta\phi$ at the respective maximal and minimal values of δU_{gel}, which are indicated by dots in (c).

sponsive case ($\chi^*=0$), where the polymer does not deform due to the chemical reaction and the BZ patches only interact through the chemical degrees of freedom. In particular, Fig. 3(b) shows that for $1\leq\Delta x\leq 3$, the nonresponsive gel is in oscillation death regime [19]. The absence of the oscillation death at $\chi^*=0.105$ allows us to conclude that the chemomechanical coupling has a stabilizing effect on the synchronized oscillations.

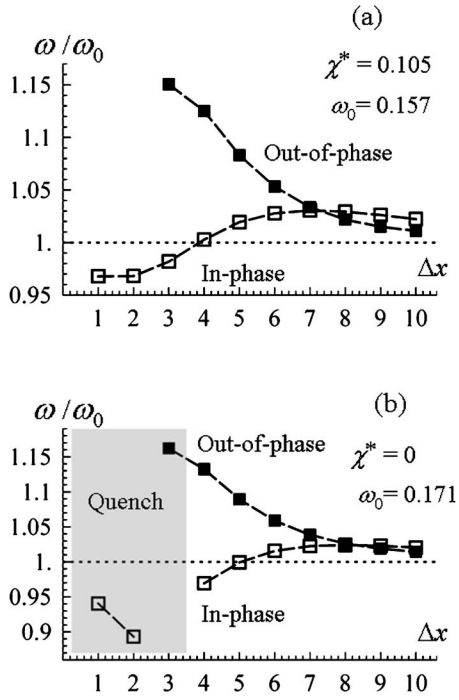

FIG. 3. The frequency of oscillations ω of the in-phase and out-of-phase synchronization modes as a function of the interpatch separation Δx. (a) Responsive gel. (b) Nonresponsive gel. ω_0 is the frequency of oscillation within an isolated patch. The shaded area in (b) indicates the domain of the oscillation death regime.

The in- and out-of-phase regimes of synchronization and the oscillation death were previously observed in experimental studies of two coupled continuously stirred tank reactor (CSTR) systems undergoing the oscillatory BZ reaction [19]. Unlike the behavior shown in Fig. 3, the frequency of oscillations in the out-of-phase regime was reported to be lower than the frequency of the uncoupled oscillations [19]. Furthermore, the frequency of the out-of-phase oscillations decreased with an increase in the coupling strength until the oscillation death occurred, and an asymmetric steady state was established in the system [19]. The difference between the behavior reported in Ref. [19] and shown in Fig. 3 could be attributed to the difference in the nature of coupling. Namely, the BZ oscillations in the two CSTRs interacted through the concentration of oxidized catalyst v [19], whereas the interaction is controlled by the activator u in the system considered here.

As can be seen from Fig. 3, for both responsive and nonresponsive heterogeneous gels, the frequency of oscillation was found to be remarkably different in the in-phase and out-of-phase regimes of synchronization at $\Delta x<7$. This implies that a theoretical analysis of the synchronization based on the phase reduction technique [15,20] is of a limited applicability to the system under consideration. This theoretical approach assumes that the oscillators are coupled so weakly that the interaction has a negligible effect on the frequency of oscillation. As evident from Fig. 3, this assumption is valid only if the patches are placed sufficiently far from each other.

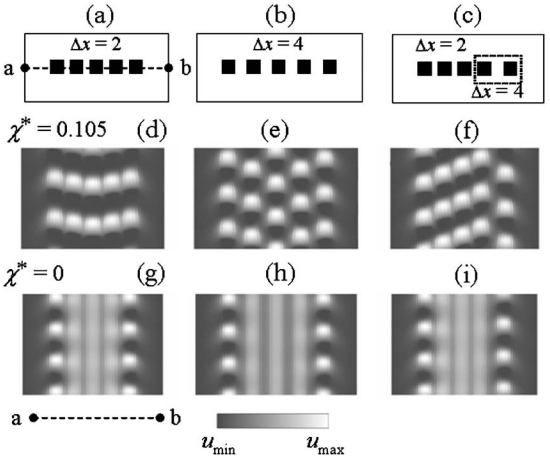

FIG. 4. Dynamical patterns in the heterogeneous gel having five catalyst patches arranged in a linear array: the effect of the interpatch spacing. [(a)–(c)] Schematics of the systems. [(d)–(i)] The spatiotemporal behavior of u along the central horizontal cross section of the sample for [(d)–(f)] responsive and (g)–(i) nonresponsive gels. The lattice spacing in the simulations is L_0. The gel dynamics is shown during a period of time of $100T_0$. Grayscale bar: $u_{\min}=8.42\times10^{-5}$, $u_{\max}=0.357$ at $\chi^*=0.105$; $u_{\min}=8.22\times10^{-5}$, $u_{\max}=0.268$ at $\chi^*=0$.

We note that the frequency of oscillations depends on the spatial-temporal behavior of the concentration u between the patches. At sufficiently small Δx, the in-phase and out-of-phase regimes exhibit quite different distributions of u in the interpatch space.

The dependencies shown in Fig. 3(a) provide valuable guidelines for designing patterned BZ gels that exhibit the desired dynamic behavior. To illustrate the utility of these design rules, we consider five catalytic patches that are arranged in a linear array. In simulations of the gels having five BZ patches, the lattice spacing was L_0, and the initial concentrations u and v were $u/\phi=v/\phi=10^{-3}$ ($v=0$ outside the patches). The evolution of the system was simulated for a period of $6000T_0$ to ensure that the developed dynamical pattern was stable.

First, we focus on situations where all the patches are placed equidistantly, with $\Delta x=2$ and $\Delta x=4$, as shown, respectively, in Figs. 4(a) and 4(b). For the two-patch case at $\Delta x=2$, only the in-phase synchronization is supported by the system [see Fig. 3(a)]. The simulations reveal that the corresponding array of five patches also exhibits the in-phase synchronization [see Fig. 4(d)]. (The pattern is slightly bent because the end patches interact only with one neighboring patch, and consequently, they exhibit a slightly higher frequency than the internal patches.)

For $\Delta x=4$, both the in- and out-of-phase modes of pairwise synchronization exist, but the out-of-phase mode has a higher frequency than the in-phase mode [Fig. 3(a)]. It is well known that in an ensemble of coupled chemical oscillators, the dynamical mode having the highest frequency always dominates [17,20–22]. It is evident from the dynamical pattern in Fig. 4(e) that at $\Delta x=4$, the neighboring patches do indeed exhibit the out-of-phase synchronization.

Finally, we consider an array of the catalyst patches where the distance between the two patches at the right end is $\Delta x=4$, while all other reactive domains are spaced at $\Delta x=2$ [Fig. 4(c)]. As anticipated from the findings in Fig. 3(a), the pair of patches at $\Delta x=4$ oscillates out of phase, with a frequency that is greater than that of the in-phase mode at $\Delta x=2$. The simulations show that this pair forms a pacemaker and thereby generates a chemical wave that propagates to the left [see Fig. 4(f)]. This wave can be harnessed to create a micropump, which drives dissolved species from one end of the sample to another.

The responsiveness of the gel to the BZ reaction is crucial for the existence of the dynamical behavior shown in Figs. 4(d)–4(f). As seen in Figs. 4(g)–4(i), a nonresponsive polymer matrix ($\chi^*=0$) will not produce the rich dynamics discussed above.

It is worth noting that after the dynamical patterns in Figs. 4(d)–4(i) were developed, they were sustained for a long time of about $5000T_0$ ($\sim$ corresponding to 1.5 h). The stability of the patterns was then tested by perturbing the concentrations u and v with a random noise (see Sec. II B). The perturbation was applied three times within the interval of $3000T_0$. The stability of the highly synchronized dynamics in the arrays of the BZ patches [Figs. 4(a)–4(c)] was found to depend on the responsiveness of the gel. For example, at $\chi^*=0.105$, the dynamic patterns in Figs. 4(d) and 4(f) exhibited no effect of the noise. In contrast, at $\chi^*=0$, the perturbations changed the behavior shown in Figs. 4(g) and 4(i) to induce a unidirectional chemical wave.

IV. CONCLUSIONS

In summary, we undertook the first studies to determine how the compartmentalization of BZ gels in a nonresponsive polymer matrix affects the dynamical behavior of the system. The results point to a "modular" design approach, which can impart the desired functionality to the material. In particular, identical pieces of BZ gel form the crucial components and it is the arrangement of these pieces that determines and provides the desired performance. For example, the out-of-phase pattern shown in Fig. 4(e) can be utilized to effectively double the operating frequency in a BZ gel-based coating that is used to sense features of the underlying surface [23]. In contrast, the wavelike swelling and deswelling motion within the responsive gel shown in Fig. 4(f) can be potentially used to pump reagents or fluid through the system, while the concerted behavior seen in Fig. 4(d) might be valuable for fabricating a microactuator. In future studies, we will extend this concept by patterning the sample with rectangular strips and by combining square patches with these rectangular pieces. This approach can be viewed as inscribing a Lego set within a polymer gel and using these inscribed components to build the desired device. The computational studies described herein provide the necessary guidelines for assembling the components into the appropriate pattern to yield the specified function.

ACKNOWLEDGMENT

Funding from ARO is gratefully acknowledged.

[1] S. Maeda, S. Hashimoto, and R. Yoshida, *Proceedings of the IEEE International Conference on Robotics and Biomimetics* (IEEE, Piscataway, NJ, 2004), p. 474; S. Maeda, Y. Hara, R. Yoshida, and S. Hashimoto, *Proceedings of the First IEEE/RAS-EMBS International Conference on Biomedical Robotics and Biomechatronics* (IEEE, Piscataway, NJ, 2006), p. 1160.
[2] R. Yoshida, Curr. Org. Chem. **9**, 1617 (2005).
[3] R. Yoshida, T. Takahashi, T. Yamaguchi, and H. Ichijo, J. Am. Chem. Soc. **118**, 5134 (1996).
[4] B. P. Belousov, *Collection of Short Papers on Radiation Medicine* (Medgiz, Moscow, 1959), p. 145; A. M. Zhabotinsky, Dokl. Akad. Nauk SSSR **157**, 392 (1964); A. N. Zaikin and A. M. Zhabotinsky, Nature (London) **225**, 535 (1970).
[5] V. V. Yashin and A. C. Balazs, J. Chem. Phys. **126**, 124707 (2007).
[6] O. Kuksenok, V. V. Yashin, and A. C. Balazs, Soft Matter **3**, 1138 (2007).
[7] V. V. Yashin and A. C. Balazs, Science **314**, 798 (2006).
[8] V. V. Yashin and A. C. Balazs, Macromolecules **39**, 2024 (2006).
[9] J. J. Tyson and P. C. Fife, J. Chem. Phys. **73**, 2224 (1980).
[10] O. Steinbock, P. Kettunen, and K. Showalter, Science **269**, 1857 (1995).
[11] A. Onuki, Adv. Polym. Sci. **109**, 63 (1993).
[12] B. Barriere and L. Leibler, J. Polym. Sci., Part B: Polym. Phys. **41**, 166 (2003).
[13] R. J. Atkin and N. Fox, *An Introduction to the Theory of Elasticity* (Longman, New York, 1980).
[14] Note that the two oscillators are identical. Therefore, the synchronization occurs at any interaction strength; see Ref. [15].
[15] A. Pikovsky, M. Rosenblum, and J. Kurths, *Synchronization. A Universal Concept in Nonlinear Sciences* (Cambridge University Press, Cambridge, 2001).
[16] L. Kuhnert, Nature (London) **319**, 393 (1986).
[17] O. U. Kheowan, E. Mihaliuk, B. Blasius, I. Sendina-Nadal, and K. Showalter, Phys. Rev. Lett. **98**, 074101 (2007).
[18] For example, illuminating the sample with high intensity, uniform light would erase the oscillatory activity in the patches. Upon switching the illumination off, the BZ oscillations in the patches would restart from the same phase. Similarly, applying light of nonuniform intensity (or screening one patch from the light) would dephase the BZ oscillations in the patches.
[19] M. F. Crowley and R. J. Field, J. Phys. Chem. **90**, 1907 (1986); M. F. Crowley and I. R. Epstein, *ibid.* **93**, 2496 (1989).
[20] Y. Kuramoto, *Chemical Oscillations, Waves, and Turbulence* (Springer-Verlag, Berlin, 1984).
[21] A. S. Mikhailov and K. Showalter, Phys. Rep. **425**, 79 (2006).
[22] H. Fukuda, N. Tamari, H. Morimura, and S. Kai, J. Phys. Chem. A **109**, 11250 (2005).
[23] B. R. Ratna (private communication).